Interaction of NADP(H) with Oxidized and Reduced P450 Reductase during Catalysis. Studies with Nucleotide Analogues†

Marat B. Murataliev* and René Feyereisen

Department of Entomology and Center for Toxicology, University of Arizona, Tucson, Arizona 85721-0036

Received December 21, 1999; Revised Manuscript Received February 17, 2000

ABSTRACT: Previous studies have shown that the interaction of P450 reductase with bound NADP(H) is essential to ensure fast electron transfer through the two flavin cofactors. In this study we investigated in detail the interaction of the house fly flavoprotein with NADP(H) and a number of nucleotide analogues. 1,4,5,6-Tetrahydro-NADP, an analogue of NADPH, was used to characterize the interaction of P450 reductase with the reduced nucleotide. This analogue is inactive as electron donor, but its binding affinity and rate constant of release are very close to those for NADPH. The 2′-phosphate contributes about 5 kcal/mol of the binding energy of NADP(H). Oxidized nicotinamide does not interact with the oxidized flavoprotein, while reduced nicotinamide contributes 1.3 kcal/mol of the binding energy. Oxidized P450 reductase binds NADPH with a K_d of 0.3 μM, while the affinity of the reduced enzyme is considerably lower, $K_d = 1.9$ μM. P450 reductase catalyzes a transhydrogenase reaction between NADPH and oxidized nucleotides, such as thionicotinamide-NADP$^+$, acetylpyridine-NADP$^+$, or [^{3}H]NADP$^+$. The reverse reaction, reduction of [^{3}H]NADP$^+$ by the reduced analogues, is also catalyzed by P450 reductase. We define the mechanism of the transhydrogenase reaction as follows: NADPH binding, hydride ion transfer, and release of the NADP$^+$ formed. An NADP$^+$ or its analogue binds to the two-electron-reduced flavoprotein, and the electron-transfer steps reverse to transfer hydride ion to the oxidized nucleotide, which is released. Measurements of the flavin semiquinone content, rate constant for NADPH release, and transhydrogenase turnover rates allowed us to estimate the steady-state distribution of P450 reductase species during catalysis, and to calculate equilibrium constants for the interconversion of catalytic intermediates. Our results demonstrate that equilibrium redox potentials of the flavin cofactors are not the sole factor governing rapid electron transfer during catalysis, but conformational changes must be considered to understand P450 reductase catalysis.

Flavoproteins play an important role in a variety of biological electron transfer processes. Unlike metalloproteins and nicotinamide nucleotides which can undergo only one- and two-electron transitions, respectively, flavin cofactors (FMN or FAD) can undergo both two- and one-electron redox transitions. NADPH-cytochrome P450 reductase (P450 reductase,[1] EC 1.6.2.4) catalyzes transfer of the reducing equivalents from the two-electron donor, NADPH, to a one-electron acceptor, cytochrome P450 (*1*). Cytochrome P450 reductase belongs to a family of flavoproteins containing both FAD and FMN as cofactors. Other members of this family are the flavoprotein domains of cytochrome P450BM3 and of nitric oxide synthase, as well as the flavoprotein subunit of sulfite reductase (*2*).

Diflavin reductases are believed to have evolved as a result of a gene fusion event between an FAD-containing flavoprotein reductase, homologous to ferredoxin:NADP$^+$ reductase, and an FMN-containing electron carrier homologous to flavodoxin (*2*). The FMN-containing flavoproteins serve as electron carriers between a number of redox enzymes. The FAD-containing reductases catalyze transfer of reducing equivalents between NAD(P)H and redox partners such as cytochromes, iron−sulfur proteins, or other flavoproteins. In chloroplasts, the ferredoxin:NADP$^+$ reductase system catalyzes NADP$^+$ reduction, while in mammalian mitochondria and endoplasmic reticulum, NADPH is oxidized to supply reducing equivalents for steroid hormone or xenobiotic metabolism by cytochrome P450 enzymes.

The crystal structure of the rat liver cytochrome P450 reductase reveals well-resolved binding of the adenine portion of NADP$^+$, while the nicotinamide moiety is not well-defined (*3*). The nicotinamide moiety is also poorly defined in the crystal structure of the homologous ferredoxin reductase (*4*, *5*). The P450 reductase structure suggested a mechanism of rapid interflavin electron transfer: the isoalloxazine rings of FAD and FMN are located less than 4 Å apart, allowing fast direct electron transfer (*3*). Transfer of the reducing equivalents between NADPH and FAD is not as obvious. In one of the conformations which is assumed to reflect a structure of the enzyme−nucleotide complex during catalysis, the nicotinamide moiety of bound NADP$^+$ is spatially separated from the isoalloxazine ring of FAD by Trp677 so

† This work was supported by National Institutes of Health Grants GM39014 and ES06694.

* To whom correspondence should be addressed at the Department of Entomology, Forbes 410, P.O. Box 210036, University of Arizona, Tucson, AZ 85721-0036. Tel.: +1 (520)-621-9547. FAX: +1 (520)-621-1150. E-mail: marat@ag.arizona.edu.

[1] Abbreviations: H_4-NADP, 1,2,5,6-tetrahydro-NADP; P450 reductase, NADPH-cytochrome P450 reductase; P450BM3, cytochrome $P450_{BM3}$, isolated from *Bacillus megaterium*; AcPy-NADP(H), 3-acetylpyridine-NADP(H); S-NADP(H), thionicotinamide-NADP(H); NMN, nicotinamide mononucleotide.

10.1021/bi992917k CCC: $19.00
Published on Web 04/04/2000

that direct rapid hydride ion transfer is unlikely. Some structural changes of the catalytic site must be associated with NADPH binding and/or hydride ion transfer.

Interaction with nicotinamide nucleotides has been shown to play an important role in catalysis by cytochrome b_5 reductase (*6*) and by the adrenodoxin reductase−adrenodoxin complex (*7*). Studies from our group have demonstrated that NADP(H) binding is essential for fast rates of catalysis by P450BM3 (*8*), and for fast reduction of cytochrome *c* by the house fly P450 reductase (*9*). Our results also suggested that changes in the enzyme's affinity to NADPH and $NADP^+$ occurring during catalysis could serve as a driving force for electron transfer (*9*). However, the mechanism of the nucleotide effect on flavin redox properties and the role of NADP(H) binding in P450 reductase catalysis remain unclear.

To gain a better understanding of the mechanism of electron transfer by P450 reductase and of the role of nucleotide binding, we characterized the interaction of NADP(H), nucleotide fragments, and nucleotide analogues with cytochrome P450 reductase from the house fly. The compounds tested were 5′-AMP, 2′-AMP, 2′,5′-ADP, 2′-ADP-ribose, and NADP(H) to determine parts of the dinucleotide responsible for high-affinity binding. An NADPH analogue, 1,2,5,6-tetrahydro-NADP was used to characterize the interaction of the enzyme with the reduced nucleotide. These results as well as the results obtained with AcPy-NADP(H) and S-NADP(H) allowed us to characterize the catalytic cycle and to estimate the steady-state distribution of catalytic intermediates.

EXPERIMENTAL SECTION

Chemicals. The following chemicals were purchased from Sigma: NAD^+ (N-1511), $NADP^+$ (N-0505), 5′-AMP (A-2002), 2′-AMP (A-9396), 2′,5′-ADP (A-5638), 2′-ATP-ribose (M-1879), AcPy-$NADP^+$ (A-1046), S-$NADP^+$ (T-5515), NMN (N-3501), cytochrome *c* (C-2506), glucose-6-phosphate (G-7250), glucose-6-phosphate dehydrogenase (G-8404), snake venom phosphodiesterase (from *Crotalus adamanteus*, P-6877). NADPH (621692) was from Boehringer Mannheim. The purity of the nucleotides was over 95% as shown by HPLC with detection at 259 nm. Palladium 5% on activated carbon was from Aldrich (20 568-0).

Enzymes. House fly (*Musca domestica* L.) P450 reductase was expressed in *E. coli* and purified using ion exchange and affinity chromatography as described earlier (*9*). Glucose-6-phosphate dehydrogenase was depleted of tightly bound $NADP^+$ as described earlier (*8*).

Binding of [^{3}H]NADP$^+$ and [^{3}H]NADPH. [^{3}H]$NADP^+$ was synthesized and purified by the procedure used for [^{32}P]-$NADP^+$ preparation (*10*). The specific activity of the purified nucleotide was 1 μCi/nmol. Binding of the radiolabeled nucleotides was carried out in a 240 μL volume in 0.1 M Tris-HCl, pH 7.7, at 25 °C. When NADPH binding was measured, the reaction mixture also contained 2 mM glucose-6-phosphate and 0.4 unit/mL of nucleotide-depleted (*8*) glucose-6-phosphate dehydrogenase. P450 reductase was incubated at 1.5−5 μM with increasing concentrations of [^{3}H]NADP(H) for 5 min, 220 μL of the reaction mixture was placed in a Microcon-30 (Amicon) microconcentrator, and the samples were centrifuged for 15 s in a Picofuge (Stratagene) centrifuge at 6000 rpm. The concentrators were then placed in the new collecting tubes and centrifuged for 60 s. The first centrifugation, which produced about 4−5 μL of eluate, was required to remove a small volume of glycerol retained in the membrane. The second centrifugation produced 15−20 μL of eluate. The radioactivity of the aliquots of the reaction mixture before and after filtration was determined by liquid scintillation counting, and the amount of bound [^{3}H]NADP(H) was calculated as a difference.

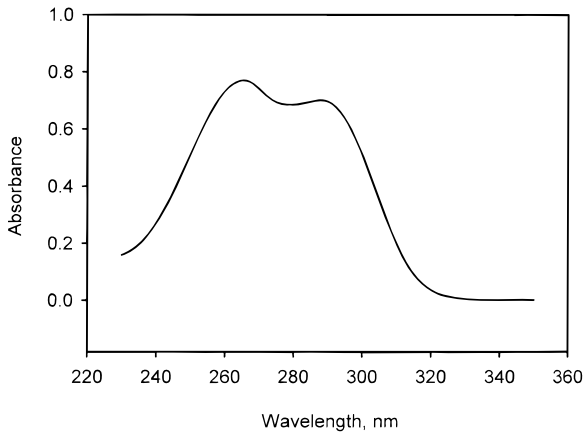

FIGURE 1: Absorption spectrum of 30 μM H_4-NADP in 0.1 M Tris-HCl, pH 7.7, buffer.

H_4NADP Synthesis. H_4NADP was synthesized by catalytic hydrogenation as described (*11*, *12*), with some modifications as follows. A reaction mixture with 0.38 mmol of $NADP^+$ and 0.69 mmol of glucose-6-phosphate in 10 mL of 10 mM Tris-HCl, pH 8.0, buffer was incubated in the presence of 10 units of glucose-6-phosphate dehydrogenase for 45 min at 35 °C. Then 100 mg of palladium catalyst was added, and the reaction mixture was incubated at 25 °C under H_2 atmosphere for 3 h with constant stirring. Formation of tetrahydropyridine was followed by UV and NMR spectroscopy. At the end of incubation, the reaction mixture was passed through a 30K ultrafiltration membrane to remove the fine charcoal suspension, diluted 10 times with water, and loaded on a 2.5 × 75 cm DEAE-cellulose column equilibrated at 4 °C with 20 mM triethylammonium bicarbonate buffer, pH 7.5. The column was developed at 45 mL/h with 250 × 250 mL of a 0.2−0.9 M linear gradient of triethylammonium bicarbonate, pH 7.5, buffer. Fractions were collected every 12 min, and the absorbance at 265 and 288 nm was measured. The fractions with a A_{265}/A_{288} ratio of ≤1.15 were pooled, and triethylammonium bicarbonate was removed by freeze-drying. The purity of the analogue was 90−95% as shown by HPLC and TLC.

Determination of the H_4NADP Extinction Coefficient. The analogue was incubated at 25 °C in 0.1 M Tris-HCl, pH 7.7, in the presence of 0.5 unit/mL of snake venom phosphodiesterase for 20 min. The reaction mixture was subjected to HPLC, and the amount of 2′,5′-ADP released was determined by comparison with a standard 2′,5′-ADP solution. An extinction coefficient of 15.4 mM^{-1} cm^{-1} was used to calculate the concentration of 2′,5′-ADP. HPLC was carried out on a Whatman Partisil 10 SAX 4.6 × 250 column isocratically developed in 0.2 M sodium phosphate, pH 6.0, at a flow rate of 1 mL/min with detection at 260 nm. The UV absorption spectrum of H_4NADP is shown in Figure 1,

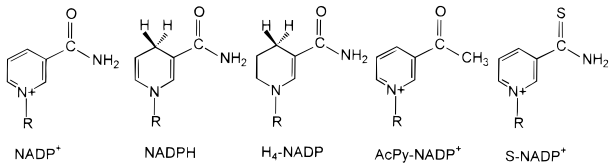

FIGURE 2: Structure of the nicotinamide moiety of NADP(H) and the analogues used.

and its structure is in Figure 2. The absorbance maximum is at 265 nm ($\epsilon = 25.3$ mM^{-1} cm^{-1}) with a shoulder at 288 nm ($\epsilon = 21.9$ mM^{-1} cm^{-1}).

Activity Assays. All assays and incubations were carried out in 0.1 M Tris-HCl, pH 7.7, buffer as described (*9*, *10*). Unless indicated otherwise, an NADPH regenerating system consisting of 2.0 mM glucose-6-phosphate and 3.0 units/mL glucose-6-phosphate dehydrogenase was used. In assays with NADPH analogues, nucleotide-depleted glucose-6-phosphate dehydrogenase (*8*) was used. Concentrations of P450 reductase, cytochrome *c*, and NADPH or its analogues were as specified in the legends.

Transhydrogenase activity was determined spectrophotometrically in the presence of 100 μM of each reduced and oxidized nucleotide and/or analogue. S-NADPH formation was measured at 395 nm using $\epsilon_{395} = 11.3$ (*13*). Formation of AcPy-NADPH was measured at 393 nm using $\epsilon_{393} = 4.55$. When transhydrogenase activity was carried out with $(1.5-2.0) \times 10^5$ dpm of [^{3}H]NADP$^+$ as electron acceptor, the reaction mixture (200 μL) contained 200 μM of each electron donor and acceptor. The reaction was terminated by addition of 20 μL of 2% SDS solution, and samples were analyzed by anion exchange HPLC as described above with an online radioactivity detector. [^{3}H]NADPH formed was calculated as a fraction of total radioactivity in the NADP$^+$ and NADPH peaks. No other radioactive product was formed during the reaction.

Other Procedures. Reduced NADP$^+$ analogues were prepared as described for [^{32}P]NADPH (*10*). P450 reductase flavin reduction was followed by the absorbance decrease at 460 nm as detailed elsewhere (*9*). EPR spectra of duplicate samples were measured as described earlier (*8*). Protein concentration was determined by the Lowry procedure (*14*) using bovine serum albumin as a standard. The molar concentration of P450 reductase was calculated based on protein content using a M_r value of 80 000 (*15*).

RESULTS AND DISCUSSION

Inhibition by P_i and PP_i. A number of observations with P450 reductases indicated that ionic strength influences nucleotide binding. High salt concentration decreased affinity to NADPH of mammalian (*16*, *17*) and insect P450 reductase (*9*). We studied the effect of inorganic phosphate and pyrophosphate on cytochrome *c* reductase activity of house fly P450 reductase in more detail. Both P_i and PP_i inhibited cytochrome *c* reduction competitively with respect to NADPH, with K_i values of 33 and 2 mM, respectively (Table 1). This suggests that both P_i and PP_i bind to the NADPH binding site. Such an effect on NADP(H) binding is expected as strong electrostatic interactions are involved in dinucleotide binding. In addition to the electrostatic effect of ionic strength, anions such as phosphate, pyrophosphate, or sulfate could specifically bind to the nucleotide binding site.

Table 1: Inhibition of the Cytochrome *c* Reductase Activity by the NADP Fragments and Analogues[a]

nucleotide fragments	K_i	ΔG_o (kcal/mol)[b]
P_i	33.3 ± 7.2 mM (3)	2.01
PP_i	2.1 ± 0.21 mM (3)	3.64
NAD	18.3 ± 4.4 mM (3)	2.36
5′-AMP	7.3 ± 0.8 mM (3)	2.91
2′-AMP	45.5 ± 8.6 μM (6)	5.90
2′,5′-ADP	4.4 ± 0.3 μM (3)	7.28
2′-ATP-ribose	2.8 ± 0.4 μM (3)	7.54
NADP$^+$	3.3 ± 0.5 μM (7)	7.45
H_4-NADP	0.4 ± 0.1 μM (3)	8.69
NADPH (K_d)[c]	0.31 ± 0.04 μM (3)	8.84
AcPy-NADP	1.5 ± 0.3 μM (3)	7.91
S-NADP	1.5 ± 0.3 μM (3)	7.91

[a] Values are means ± SD of (*n*) experiments. [b] ΔG_o: Gibb's free energy changes for the binding of nucleotides. [c] K_d for NADPH from (*9*).

Inhibition of Cytochrome c Reduction by Nucleotide Fragments. We studied the inhibition of cytochrome *c* reductase activity by a number of nucleotides to determine the contribution of the separate parts of NADP(H) in binding. NMN at 20 mM produced no detectable inhibition, and this compound was not analyzed further. All other compounds served as competitive inhibitors with respect to NADPH, as was previously shown for NADP$^+$ and 2′-AMP (*9*). The results are summarized in Table 1.

NAD$^+$ and 5′-AMP inhibited cytochrome *c* reduction with a K_i in the millimolar range, similar to P_i and PP_i. Nucleotides with a 2′-phosphate at the adenine ribose were much more potent inhibitors with a K_i for 2′-AMP of 44 μM. The affinity increased by an order of magnitude by the addition of a 5′-phosphate as in 2′,5′-ADP. No significant increase in binding affinity was observed for 2′-ATP-ribose, suggesting that the second phosphate and nicotinamide ribose of NADP(H) do not contribute significantly to binding. Surprisingly, only a marginal effect was observed for NADP$^+$ compared to 2′-ATP-ribose. This is consistent with the lack of inhibition by NMN. These data suggested that the positively charged nicotinamide ring does not contribute to the binding of the oxidized dinucleotide to the oxidized P450 reductase.

H_4NADP. To explore nicotinamide binding, we prepared an analogue of the reduced nucleotide, 1,4,5,6-tetrahydro-NADP (H_4NADP). This compound is inactive as an electron donor and carries no positive charge in the pyridinium ring, thus being an analogue of NADPH rather than NADP$^+$. Molecular modeling revealed that the pyridinium ring of H_4NADP had a 3-dimensional structure very close to that of NADPH (data not shown). Figure 2 shows the structures of NADP$^+$, NADPH, and H_4NADP.

H_4NADP inhibited cytochrome *c* reductase activity competitively with respect to NADPH. Measurements of the inhibition constant demonstrated that the analogue binds to the enzyme 8 times stronger than NADP$^+$ (Table 1), while its affinity of 0.4 μM is close to that for NADPH [K_d = 0.31 μM, (*9*)]. Thus, we conclude that H_4NADP binds to the enzyme like a substrate, NADPH.

This demonstrates that P450 reductase binds reduced and oxidized dinucleotides with different affinities, as a result of a differential interaction of the reduced and oxidized nicotinamide with the enzyme. The nicotinamide moiety of NADP$^+$ does not interact with the enzyme, while that of

Table 2: Contribution of Different NADP(H) Fragments in Binding

residue	$\Delta\Delta G_o$ (kcal/mol)	$NADP^+$ (%)	NADPH (%)
5′-phosphate (2′,5′-ADP vs 2′-AMP)	1.38	18.5	15.6
2′-phosphate (NADP vs NAD)	4.37	58.7	49.4
2′-phosphate (5′-AMP vs 2′,5′-ADP)	5.09	68.3	57.6
PP-ribose$_{nic}$[a] (ATP-R vs 2′-AMP)	1.64	22.0	18.6
P-ribose$_{nic}$ (ATP-R vs 2′5′-ADP)	0.26	3.5	2.9
oxidized nicotinamide ($NADP^+$ vs ATP-R)	−0.09	−1.2	−
reduced nicotinamide (NADPH vs ATP-R)	1.30	−	14.7

[a] Subscript "nic" designates ribose of the nicotinamide portion of dinucleotide.

NADPH contributes significantly to high-affinity binding. The pyridinium rings of the reduced and oxidized nucleotides have three differences: the C4 of the reduced nucleotide carries an extra hydrogen; the reduced nicotinamide is flat but assumes a boat conformation when oxidized; the reduced nicotinamide does not have a positive charge at N1. Because P450 reductase affinities for H_4NADP and NADPH are very close despite the presence of two extra hydrogens in the analogue, and because of the relatively large affinity difference between reduced and oxidized nucleotides, we conclude that the nicotinamide charge is the most important factor in recognition between $NADP^+$ and NADPH. A similar conclusion has been reached for alcohol dehydrogenase, where the phenyl and pyridinium analogues of NAD(H) differing by charge but not conformation have a 100-fold difference in affinity (*18*).

Contribution of Different Moieties of NADP(H) in Binding. Analysis of the K_i values (Table 1) allowed us to estimate the contributions of different parts of NADP(H) in binding (Table 2). It is obvious that compounds with no 2′-phosphate at the adenine ribose interact with the house fly P450 reductase only poorly. The contribution of the 2′-phosphate can be estimated from comparisons of 5′-AMP with 2′,5′-ADP and of $NADP^+$ with NAD^+. In both cases, about 10 000-fold increase in affinity, equivalent to about 5 kcal/mol of binding energy, was observed. The contribution of the 2′-phosphate to binding is therefore about 50−60% of the total free energy change.

A comparison of 2′-AMP and 2′,5′-ADP shows that the 5′-phosphate contributes 1.4 kcal/mol in nucleotide binding, which constitutes 15−18% of the binding energy. The pyrophosphate bridge and nicotinamide ribose contribute about 20% of the binding energy, which is mainly due to the interaction with the 5′-phosphate of adenine ribose, while the contribution of the nicotinamide ribose-phosphate is minor. Indeed, the affinities of 2′,5′-ADP and ATP-R are very close to that observed for $NADP^+$, while no inhibition is observed with NMN. The positively charged nicotinamide of $NADP^+$ does not interact with the enzyme, or slightly destabilizes interaction of the adenine part of the dinucleotide. In contrast, the neutral nicotinamide of the reduced dinucleotide (NADPH or H_4NADP) contributes 1.3 kcal/mol, or about 15% of the binding energy, and increases affinity by almost an order of a magnitude.

Our previous studies on the nucleotide specificity of P450 reductase demonstrated that NADP(H) interaction with the enzyme is essential to ensure fast electron transfer through the flavin cofactors (*9*). NADH which lacks the 2′-phosphate did not support high rates of electron transfer. The present results show that P450 reductase interaction with the 2′-phosphate of the adenine ribose is the major contributor to high-affinity binding and fast hydride ion transfer. This implies that 2′-phosphate is important for interaction of the nicotinamide ring of NADPH with the electron acceptor, FAD.

Our results also imply that the primary nucleotide recognition occurs at the adenine part, 2′-phosphate ensures tight binding, and induces some conformational changes to facilitate binding of the nicotinamide portion of the reduced dinucleotide. Such an idea is corroborated by our results of mutagenesis of the C560 residue of P450 reductase, which is located just 4 Å away from the adenine ribose in the structure of the mammalian P450 reductase (*3*). The C560Y mutation of the insect enzyme significantly decreased the affinity of NADP(H) binding, with little if any effect on the binding of 2′-AMP (*9*). It also appears that interaction of 2′-phosphate with the enzyme contributes in the recognition of reduced and oxidized nicotinamide. The C560Y mutation increased both K_m and K_d for NADPH by a factor of 35, while the affinity to $NADP^+$ decreased only 8.5-fold (*9*). Considering the distance between the P atom of 2′-phosphate and N5 of FAD of 18.6 Å (*3*), the signal of the 2′-phosphate interaction with the protein must be transferred to the FAD site via conformational changes involving C560.

Such a distant conformational effect was also observed for isocitrate dehydrogenase (*19*). The crystal structure reveals that the adenine 6-NH_2 group binds >12 Å away from the hydride ion transfer site. When a hypoxanthine analogue of $NADP^+$, which has a 6-OH group in the adenine ring, is used as electron acceptor, hydride ion transfer is 2.6×10^4 times slower than with $NADP^+$.

The affinities of the house fly P450 reductase to $NADP^+$ and NAD^+ and the contribution of the 2′-phosphate are comparable to those reported for the rat liver P450 reductase (*20, 21*). However, a more detailed comparison is not possible for two reasons. First, to our knowledge no detailed analysis with other nucleotide analogues and fragments has been carried out with the mammalian flavoprotein. Second, most of the experiments with mammalian P450 reductase were carried out in the presence of up to 300 mM potassium phosphate, which interferes with the binding of both oxidized and reduced nucleotides. However, our results agree well with the results of Batie and Kamin (*22*) obtained with ferredoxin:$NADP^+$ reductase, homologous to P450 reductase: the 2′-phosphate is essential for high-affinity binding, while neither nicotinamide ribose nor nicotinamide of the oxidized nucleotide increased the affinity.

NADP(H) Binding. The number of nucleotide binding sites and the affinity of the enzyme to $NADP^+$ and NADPH were measured by a microfiltration technique as described under Experimental Section. A typical Scatchard plot of [^{3}H]-nucleotide binding is shown in Figure 3. The enzyme has one $NADP^+$ binding site with an affinity of 1.3 ± 0.4 (6) μM, which is in good agreement with the value of the inhibition constant in cytochrome *c* reduction (Table 1).

Similar measurements in the presence of glucose-6-phosphate and dehydrogenase to reduce the nucleotide gave

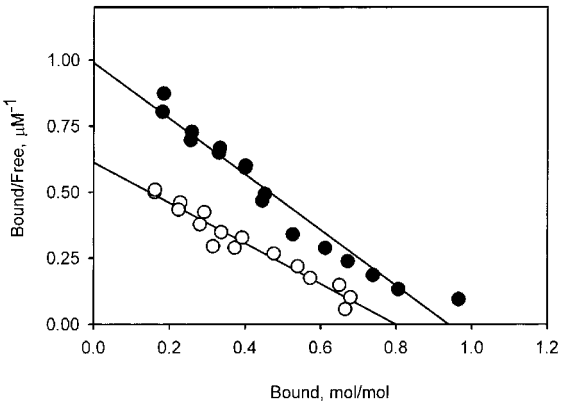

FIGURE 3: Scatchard plot of [^{3}H]NADP$^+$ and [^{3}H]NADPH binding by P450 reductase. 4.6 μM P450 reductase, 1−15 μM nucleotide, NADP$^+$ (closed circles), or NADPH (open circles). Lines are linear regression through the points. From this graph, the K_d for NADP$^+$ is 0.95 μM ($r^2 = 0.95$), and the K_d for NADPH is 1.3 μM ($r^2 = 0.95$).

a K_d for NADPH of 1.9 ± 0.6 (5) μM, in contrast to the value of 0.31 μM measured earlier by kinetic means (*9*), and to a K_i of 0.4 μM obtained for H_4NADP (Table 1). We analyzed the [^{3}H]nucleotide content in the reaction mixture used for binding studies. It was found that in the presence of 3 μM P450 reductase and an NADPH-regenerating system, all of the nucleotide is present as NADPH, and under these conditions the enzyme is reduced as confirmed by the absorption spectrum (data not shown). Thus, the K_d value of 1.9 μM derived from the Scatchard plot represents the interaction of the reduced nucleotide with the reduced enzyme, while oxidized P450 reductase binds NADPH considerably tighter, with a K_d in the range of 0.3−0.4 μM. This has also been observed for oxidized ferredoxin reductase and adrenodoxin reductase which bind NADPH with considerably higher affinity than NADP$^+$ (*7*, *22*).

The following observations also demonstrate that P450 reductase interaction with NADP(H) depends on the state of flavoprotein reduction. Neither P450 reductase (*10*) nor the flavoprotein domain of P450BM3 (*8*) can rapidly accept reduced equivalents from NADPH when partially reduced, while reduction of the oxidized flavoproteins by NADPH is orders of magnitude faster (*8*, *9*, *23*, *24*). The nicotinamide portion of NADP$^+$ does not interact with the oxidized P450 reductase (Table 2). In contrast, reduced P450 reductase binds NADP$^+$ in such a way that hydride ion transfer from $FADH_2$ to the nicotinamide occurs, resulting in a transhydrogenase reaction (see below, Table 4). It should also be noted that a diazotized derivative of 3-aminopyridine-ADP covalently modified rat liver P450 reductase only after flavoprotein reduction by NADPH (*25*).

The nicotinamide moiety of NADP$^+$ is not well-defined in the crystal structures of P450 reductase, nor in those of ferredoxin reductase and glutathione reductase (*3*, *5*, *26*). Attempts to obtain a crystal structure of the reduced wild-type FNR with NADPH did not produce a defined density of the reduced nicotinamide (*27*). Our interpretation of these observations is that the structures of the complexes of oxidized flavoprotein with oxidized nucleotide, or reduced flavoprotein with reduced nucleotide, are not analogous to the catalytic intermediates—namely, reduced nucleotide and oxidized flavoprotein, or oxidized nucleotide with partially reduced flavoprotein.

Inhibition by NADP$^+$ Analogues. A number of analogues of nicotinamide dinucleotides have been synthesized and characterized (*28*). Some of them are active as hydride ion donors/acceptors in enzymatic reactions, although their redox potentials are different from those of natural nucleotides. We studied these analogues as electron donors and inhibitors of cytochrome *c* reduction, and as hydride ion donors and acceptors in a transhydrogenase reaction. The redox potentials of S-NADPH and AcPy-NADPH were taken from (*29*, *30*). Oxidized analogues served as competitive inhibitors of cytochrome *c* reduction with respect to NADPH. The inhibition constants are summarized in Table 1. Minor modifications at the nicotinamide ring (S-NADP$^+$ and AcPy-NADP$^+$, Figure 2) had little effect on the inhibitory properties of the nucleotides.

NADPH Analogues as Electron Donors. The reduced analogues were prepared by incubation with glucose-6-phosphate and glucose-6-phosphate dehydrogenase. Absorption spectra and HPLC analysis confirmed reduction of the nucleotides. S-NADPH, AcPy-NADPH, and NADH served as electron donors in cytochrome *c* reductase reaction, although the K_m values and maximal rates varied considerably (Table 3). None of the nucleotides was as efficient as NADPH in reducing flavin cofactors or cytochrome *c*. AcPy-NADPH showed significantly impaired K_m and V_{max} compared to NADPH. The hydride ion transfer rate and V_{max} were close to those observed with NADH, but AcPy-NADPH bound about 2000 times tighter than NADH. S-NADPH bound somewhat tighter than NADPH, but catalysis rates were about 3 times slower.

These experiments also address the relationship between the redox potential of the nucleotide and its ability to serve as electron donor. Evidently, there is little correlation between the redox potential of the nucleotide and the rate of cytochrome *c* reduction (Table 1). According to the Nernst equation, a 29 mV difference in the redox potential for hydride ion transfer corresponds to a 10-fold change in the equilibrium constant of the step. Thus, the equilibrium constants of hydride ion transfer ($FADH_2$/FAD) from S-NADPH and AcPy-NADPH decrease 16- and 330-fold, respectively, while the rate of cytochrome *c* reduction decreases only by a factor of 2.6 and 6.7, respectively, and the rate constants of hydride ion transfer decreased 3.9 and 5.7 times, respectively. This demonstrates that electron transfer from NADPH to an electron acceptor through the FAD and FMN cofactors is not governed solely by the equilibrium redox potential. Other, yet to be determined, factors control electron transfer in P450 reductase as well.

Transhydrogenase Reaction and Reversibility of Hydride Ion Transfer. Because the FAD domain of the P450 reductase is evolutionarily homologous to ferredoxin:NADP$^+$ reductase, an enzyme in which NADP$^+$ and NADPH are the physiological substrate and product, respectively, we thought that this ancestral function might be conserved in P450 reductase.

To assess the reversal of the hydride ion transfer step between NADPH and FAD, we first used S-NADP$^+$ and AcPy-NADP$^+$ as electron acceptors. Both dinucleotides have spectral properties that allow continuous spectrophotometric measurement of the transhydrogenase reaction, at 400 and 393 nm for S-NADP and AcPy-NADP, respectively. The reaction was carried out in the presence of 100 μM each

Table 3: K_m and V_{max} for NADPH and Analogues in Cytochrome *c* Reduction[a]

nucleotide	E_o (mV)[b]	V_{max} (s^{-1})	K_m (μM)	k_{+1} (M^{-1} s^{-1})[c]	k_{H2} (s^{-1})[d]
AcPy-NADPH	−248	7.5 ± 0.3 (3)	5.5 ± 0.9 (3)	1.4×10^6	5.1 ± 0.1 (4)[e]
S-NADPH	−285	18.9 ± 2.9 (3)	0.38 ± 0.13 (3)	5.0×10^7	7.6 ± 1.1 (9)[e]
NADPH	−320	50.4 ± 6.0 (6)	0.96 ± 0.16 (6)	5.2×10^7	29.3 ± 1.3 (4)[e]
NADH	−320	6.7 ± 1.0 (5)	9140 ± 2510 (5)	7.3×10^2	3.3 ± 0.2 (8)

[a] Values are means ± SD of (*n*) experiments. [b] Redox potentials are from *(16−18)*. [c] k_{+1} was calculated as the ratio V_{max}/K_m. [d] k_{H2} is the rate constant of the hydride ion transfer step. [e] Stopped-flow measurements were carried out with 5 μM HFR and 50 μM nucleotide analogue (final concentrations) at 460 nm.

Table 4: Transhydrogenase Activities Catalyzed by P450 Reductase with Different Donor and Acceptor Pairs[a]

donor	acceptor	V_{max} (s^{-1})
NADPH	AcPy-$NADP^+$[b]	1.15 ± 0.04 (3)
	S-$NADP^+$[b]	3.43 ± 0.38 (3)
	[^{3}H]$NADP^+$[c]	5.69 ± 0.63 (3)
AcPy-NADPH	[^{3}H]$NADP^+$[c]	0.75 ± 0.05 (3)
S-NADPH	[^{3}H]$NADP^+$[c]	1.59 ± 0.20 (3)

[a] Values are means ± SD of (*n*) experiments. [b] −100 μM of each nucleotide. [c] −200 μM of each nucleotide.

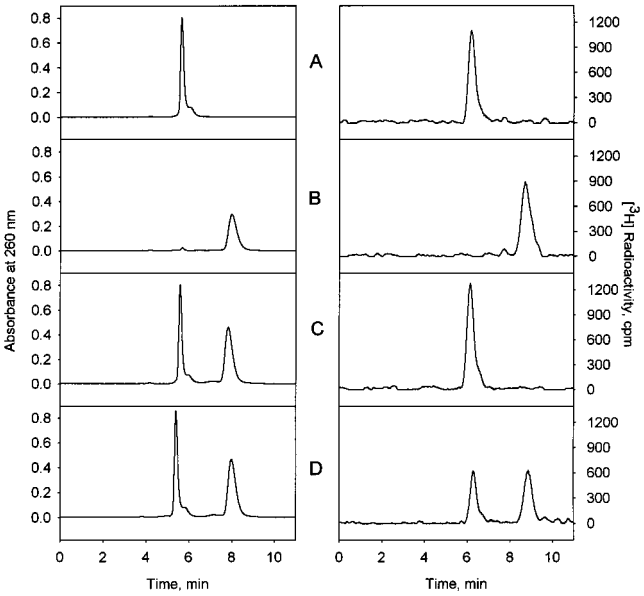

FIGURE 4: Demonstration of the NADPH → [^{3}H]$NADP^+$ transhydrogenase activity catalyzed by P450 reductase. Left panels: HPLC elution profiles monitored at 260 nm. Right panels: ^{3}H elution profile. (A) $NADP^+$; (B) NADPH; (C) mixture of $NADP^+$ and NADPH; (D) mixture of $NADP^+$ and NADPH after 10 min incubation in the presence of 0.5 μM P450 reductase.

NADPH and analogue. No detectable transhydrogenase activity was found in the absence of P450 reductase, but rapid reduction of the analogues occurred in the presence of P450 reductase (Table 4). The reaction rates with S-$NADP^+$ and AcPy-$NADP^+$ as electron acceptors are shown in Table 4.

We also investigated if P450 reductase could catalyze a transhydrogenase reaction between NADPH and $NADP^+$. The enzyme was incubated in the presence of unlabeled NADPH and [^{3}H]$NADP^+$, and, after enzyme inactivation by SDS, the nucleotides were separated by HPLC. Figure 4 shows the elution profiles of ^{3}H-labeled nucleotides and of the reaction mixture after incubation with P450 reductase. Clearly, P450 reductase catalyzes hydride ion transfer between NADPH and [^{3}H]$NADP^+$. Similar experiments using S-NADPH or AcPy-NADPH as electron donors and

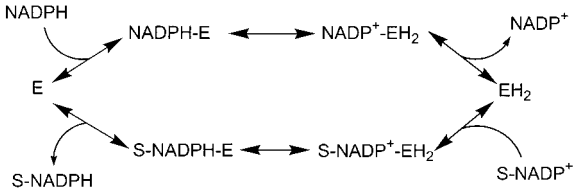

FIGURE 5: Suggested mechanism of transhydrogenase reaction catalyzed by P450 reductase. The scheme shows the reaction with S-$NADP^+$ as the acceptor. E represents oxidized enzyme. EH_2 represents a two-electron-reduced P450 reductase, independent of what flavin cofactor these electrons are residing at.

[^{3}H]$NADP^+$ as electron acceptor confirmed that transhydrogenase reaction occurs with these redox partners. The turnover numbers are presented in Table 4.

Coupling of the transhydrogenase activity was estimated by measurements of NADPH oxidase activity in the presence or absence of $NADP^+$ analogues. The turnover number for the NADPH oxidase activity was 0.08 s^{-1} in the absence of nucleotide analogue, while addition of S-$NADP^+$ increased this rate to a value of 3.6 s^{-1}, which is close to the rate of analogue reduction of 3.4 s^{-1} (Table 4). This means that in the presence of an oxidized nucleotide most of the reducing equivalents delivered to P450 reductase are utilized in the transhydrogenase reaction.

The analogues, S-NADP(H) and AcPy-NADP(H), undergo the same redox transitions as NADP(H), that is, two-electron oxidation−reduction by hydride ion transfer (*28*). Reduction of the nucleotides by P450 reductase requires transfer of 2 reducing equiv to the bound analogue. We have recently shown that P450 reductase is unable to accept more than two electrons with a catalytically competent rate (*10*). We thus conclude that the transhydrogenase reaction involves $NADP^+$ or an analogue reduction by the active, two-electron-reduced P450 reductase, which can exist in three possible states: fully reduced FMN or fully reduced FAD, and double semiquinone form.

NADPH−AcPy-$NADP^+$ reductase (transhydrogenase) activity has been used in several studies to characterize FAD-dependent activities of P450 reductase (*31, 32*). However, no mechanism has been defined for this reaction. We propose that the mechanism of the transhydrogenase reaction is as follows (Figure 5). P450 reductase binds NADPH and accepts two electrons, and $NADP^+$ is released. An $NADP^+$ or its analogue will bind to the two-electron-reduced protein, and electron-transfer reactions described above for NADPH will reverse to transfer hydride ion to the bound oxidized nucleotide, which is released and accumulates in the medium.

The experimental facts supporting this mechanism are as follows: (1) NADP(H) and analogues are obligatory two-electron donors/acceptors. (2) P450 reductase has one nucleotide binding site (Figure 3). (3) The analogues bind

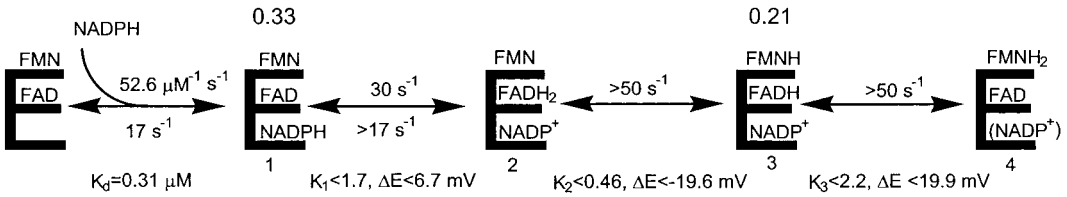

FIGURE 6: Distribution of P450 reductase species during catalysis calculated based on the experimental results. Enzyme complexes emerging after NADPH binding are numbered 1 through 4. The numbers above the complexes represent the fraction of the enzyme present as the complex. $NADP^+$ in complex 4 is in parentheses because no evidence is available whether this complex retains bound nucleotide. See text for details.

at the NADPH binding site because they are competitive inhibitors of P450 reductase with respect to NADPH. It was also shown earlier that AcPy-$NADP^+$, like $NADP^+$ and 2′,5′-ADP, protects an NADP(H) binding site lysine from chemical modification (*33*). (4) The presence of the FAD cofactor alone is sufficient to support the reaction (*21, 32*), indicating that the transhydrogenase reaction occurs at the NADP(H) binding site.

The transhydrogenase activity catalyzed by P450 reductase demonstrates that reducing equivalents of the two-electron-reduced enzyme can move rapidly between the flavin cofactors in either the forward or the reverse direction. This novel observation is not expected from the equilibrium redox potentials measured for P450 reductase and the flavoprotein domain of P450BM3 (*34, 35*). It supports our idea that, during catalytic turnover, the equilibrium redox potentials are not the major factor governing distribution of the reducing equivalents between various redox centers of P450 reductase. The proposed mechanism of the transhydrogenase reaction also implies that the function of the ancestral ferredoxin reductase, that is, reduction of $NADP^+$, is well preserved in P450 reductase.

Rate of NADPH Release. The fact that house fly P450 reductase catalyzes a relatively rapid transhydrogenase reaction highlights the importance of the rate of NADPH release from the catalytic site. The following approach was used to estimate the rate of reduced nucleotide release from the catalytic site. The enzyme was incubated with 20 μM H_4NADP and then mixed in the stopped-flow spectrophotometer with 350 μM NADPH. Under these experimental conditions, as the bound analogue is released, NADPH present in excess will bind and reduce the flavoprotein. The rate of flavin reduction will be determined by the rate of analogue release if it is slower than the hydride transfer and nucleotide binding steps. The measurements gave a value of about 21.0 ± 0.5 s^{-1}. Without prior incubation with the analogue, the rate constant for this enzyme preparation was 29.3 ± 1.3 s^{-1} (Table 2), in good agreement with the value reported previously (*9*). Thus, the rate of flavin reduction after H_4NADP binding is determined by the rate of analogue release.

The rate of H_4NADP release of 21 s^{-1} is consistent with the results of our kinetic studies (*9*). The bimolecular rate constant of NADPH binding, k_1, is 5.25×10^7 M^{-1} s^{-1}, and the K_d for NADPH was determined as 0.31 μM (*9*). As $K_d = k_{-1}/k_1$, the rate constant of NADPH release, k_{-1}, can be calculated as 16.9 s^{-1}, which agrees well with the value measured for H_4NADP.

This supports the above conclusion that H_4NADP interacts with P450 reductase as a close isosteric analogue of NADPH, and the affinity of oxidized P450 reductase to NADPH is about 0.3−0.4 μM, in contrast to the affinity of the two-electron-reduced enzyme to the reduced nucleotide which is about 1.9 μM.

EPR Measurements of Flavin Semiquinone Content. We have used EPR spectroscopy previously to demonstrate flavin semiquinone formation by the house fly P450 reductase (*9, 10*). We now measured a flavin semiquinone content of 0.42 mol of free radical/mol of enzyme under experimental conditions similar to those of the transhydrogenase reaction with NADPH as electron donor. Because the maximal reduction state of the enzyme does not exceed 2 (*10*), this value implies that a 0.21 fraction of the enzyme is present as double semiquinone, while the rest of the flavoprotein is present as either FAD or FMN hydroquinone forms.

Flavin semiquinone content was also measured with NADPH analogues which have more positive redox potentials (see Table 3). Very close semiquinone contents of 0.47 and 0.49 mol/mol of enzyme were obtained when S-NADPH or AcPy-NADPH, respectively, were used as electron donors. This unexpected finding provides additional evidence that equilibrium redox potentials are not the only factors controlling the redox properties of flavin cofactors.

Dynamic Equilibrium of Catalytic Intermediates. Measurements of transhydrogenase activity and flavin semiquinone content enabled us to estimate the fractional distribution of P450 reductase species during catalysis (Figure 6). The rate of NADPH release is 17 s^{-1} (see above), while NADPH−[^{3}H]$NADP^+$ transhydrogenase turnover is 5.7 s^{-1} (Table 4). The ratio of the two rates, $5.7/17 = 0.33$, determines the fraction of the enzyme present as a complex with NADPH bound (complex 1), while the rest of the enzyme (0.67) represents the sum of the double semiquinone and the two hydroquinone (FAD or FMN) forms.

The results of EPR measurements presented above demonstrated that 0.21 of the enzyme is present as the double semiquinone form. The sum of complexes 1 and 3 is 0.54. Therefore, the sum of complexes 2 and 4 is 0.46. The following calculations allow us to set limits on equilibrium constants and to estimate the rate constant of the individual reaction steps. Assuming that complex 4 ≫ complex 2, K_3 can be calculated as ≤2.2. If complex 4 ≪ complex 2, $K_1 \leq 2.2$, and $K_2 \leq 0.46$. The rate constant of hydride ion transfer to FAD is about 30 s^{-1} [see above and Murataliev et al. (*9*)], and the reverse rate constant can be calculated as $k_{-1} \geq 17.6$ s^{-1}. The forward rate constants k_2 and k_3 are each ≥50 s^{-1}, based on the maximal rate of cytochrome *c* reduction which is limited by hydride ion transfer (*9*).

Equilibrium constants of redox reactions can be converted into the redox potential changes using the Nernst equation. One order of magnitude change in K_{eq} corresponds to a 29 mV redox potential change for a two-electron reaction, and

to a 58 mV change for a one-electron transition. This allows us to estimate the redox potential changes of the P450 reductase with the ligands (NADP(H), FAD, and FMN) bound as follows:

$$(NADPH+FAD)/(NADP^{+}+FADH_2) < 6.7\ mV$$

$$(FADH_2+FMN)/(FADH+FMNH) < -19.6\ mV$$

$$(FADH+FMNH)/(FAD+FMNH_2) < 19.9\ mV$$

For the sake of simplicity, we only show those enzyme ligands that undergo redox transitions. It should be emphasized that these values reflect redox potential changes of the flavoprotein with NADP(H) bound. Importantly, these values indicate that catalytic steps are not associated with major free energy changes, and must be easily reversible, which is confirmed by the observed transhydrogenase activity (Table 4). On the other hand, these values are quite different from those determined by redox equilibrium titrations of mammalian P450 reductase (*34*) or P450BM3 flavoprotein (*35*). Two major differences in the approaches may explain the differences. The slow time scale in equilibrium titration measurements could lead to conformational changes of the flavoprotein and alterations of the redox properties of flavin cofactors. For example, a so-called "air-stable" FMN semiquinone could be formed, which, in house fly P450 reductase, is different from the catalytically competent FMN semiquinone (*10*). P450BM3 is also known to form an inactive three-electron-reduced flavoprotein (*36, 37*). Second, titration experiments are done in the absence of nucleotide whose binding is now known to be essential for normal catalysis.

NADPH and NADH have the same redox potentials, but the former supports much faster catalysis rates (*9*). No correlation exists between redox potentials of the analogues and their ability to support catalysis (Table 3). The redox potential of the NADPH analogues has little if any effect on the formation of a double semiquinone intermediate. These observations demonstrate that equilibrium redox potentials are not the major factor governing electron transfer. A similar conclusion has been reached recently in the study of *p*-hydroxybenzoate hydroxylase interaction with analogues of NADPH and FAD (*38*). Moreover, an FMN semiquinone form of NO synthase supports NO synthesis (*39*) despite that fact that the midpoint potential of the FMN semiquinone is −49 mV (*40*), while that of the arginine-bound heme is −220 mV (*41*).

We propose that conformational changes induced by NADP(H) interaction with P450 reductase may alter the equilibrium redox potentials of the flavin cofactors. Such a phenomenon has been demonstrated with model compounds, e.g., a flavin attached to nicotinamide by a linker of different length (*42*). In those experiments, a shorter linker increased the redox potential of the flavin by as much as 116 mV. In addition, mutagenesis of flavodoxin demonstrated that a redox potential change can be achieved by relatively minor changes of the protein: substitution of a single Gly61 residue changed the redox potential of one-electron transitions by up to 180 mV (*43*). Insertion of a more hydrophobic amino acid resulted in a larger redox potential change. In other words, relatively minor conformational changes may lead to a rather large shift of the redox potential of a flavin cofactor.

Analysis of the crystal structure of the rat P450 reductase (*3*) indicates that reduced nicotinamide should bind deep in the hydrophobic environment of the FAD isoalloxazine binding site for rapid hydride ion transfer to occur. A change of the NADPH redox potential is possible upon transfer of the neutral reduced nicotinamide from aqueous media to the hydrophobic environment of the enzyme catalytic site. Indeed, as was recently shown, the standard redox potential of the $NADP^{+}$/NADPH pair in the catalytic site of the energy-dependent transhydrogenase is shifted by +60−70 mV compared to that of the nucleotide in solution (*44*). A similar phenomenon is known to occur upon substrate(s) binding at the catalytic site of ATP synthase [see (*45*) for a review]: the free energy of ATP hydrolysis at the catalytic site is close to zero, compared to 7−8 kcal/mol in aqueous solution.

ACKNOWLEDGMENT

EPR spectra were obtained with the assistance of Dr. Arnold Raitsimring of the Department of Chemistry, University of Arizona. We thank Drs. Reddy B. Aavula and E. A. Mash of the Synthetic Core, Southwest Environmental Health Science Center (ES 06694), for their help and advice in the synthesis and NMR analysis of H_4-NADP.

REFERENCES

1. Backes, W. L. (1993) NADPH-cytochrome P450 reductase: Function in *Cytochrome P450* (Schenkman, J. B., and Greim, H., Eds.) pp 15−34, Springer-Verlag, New York.
2. Porter, T. D. (1991) *Trends Biochem. Sci. 16*, 154−158.
3. Wang, M., Roberts, D. L., Paschke, R., Shea, T. M., Masters, B. S. S., and Kim, J. J. P. (1997) *Proc. Natl. Acad. Sci. U.S.A. 94*, 8411−8416.
4. Karplus, P. A., Daniels, M. J., and Herriott, J. R. (1991) *Science 251*, 60−66.
5. Serre, L., Vellieux, F. M. D., Medina, M., Gomez-Moreno, C., Fontecilla-Camps, J. C., and Frey, F. (1996) *J. Mol. Biol. 263*, 20−39.
6. Iyanagi, T. (1977) *Biochemistry 16*, 2725−2730.
7. Lambeth, J. D., and Kamin, H. (1976) *J. Biol. Chem. 251*, 4299−4306.
8. Murataliev, M. B., Klein, M., Fulco, A. and Feyereisen, R. (1997) *Biochemistry 36*, 8401−8412.
9. Murataliev, M. B., Ariño, A., Guzov, V. M., and Feyereisen, R. (1999) *Insect Biochem. Mol. Biol. 29*, 233−242.
10. Murataliev, M. B., and Feyereisen, R. (1999) *FEBS Lett. 453*, 201−204.
11. Dave, K. G., Dunlap, R. B., Jain, M. K., Cordes, E. H., and Wenkert, E. (1968) *J. Biol. Chem. 243*, 1073−1074.
12. Wenkert, E., Dave, K. G., Haglid, F., Lewis, R. G., Oishi, T., Stevens, R. V., and Terashima, M. (1968) *J. Org. Chem. 33*, 747−753.
13. Rydström, J (1979) *Methods Enzymol. 55*, 261−275.
14. Lowry, O. H., Rosebrough, N. J., Farr, A. L., and Randall., R. J. (1951) *J. Biol. Chem. 195*, 265−275.
15. Andersen, J. F., Utermohlen, J. G., and Feyereisen, R. (1994) *Biochemistry 33*, 2171−2177.
16. Phillips, A. H., and Langdon, R. G. (1962) *J. Biol. Chem. 237*, 2652−2660.
17. Sem, D. S., and Kasper, C. B. (1995) *Biochemistry 34*, 12768−12774.
18. Danenberg, P. V., Danenberg, K. D., and Cleland, W. W. (1978) *J. Biol. Chem. 253*, 5886−5887.
19. Mesecar, A. D., Stoddard, B. L., and Koshland, D. E., Jr. (1997) *Science 277*, 202−206.
20. Sem, D. S., and Kasper, C. B. (1993a) *Biochemistry 32*, 11539−11547.

21. Sem, D. S., and Kasper, C. B. (1993b) *Biochemistry 32*, 11548−11558.
22. Batie, C. J., and Kamin, H. (1986) *J. Biol. Chem. 261*, 11214−11223.
23. Munro, A. W., Daff, S., Coggins, J. R., Lindsay, J. G., and Chapman, S. K. (1996) *Eur. J. Biochem. 239*, 403−409.
24. Sevrioukova, I., Shaffer, C., Ballou, D. P., and Peterson, J. A. (1996) *Biochemistry 35*, 7058−7068.
25. Ebel, R. E. (1981) *Arch. Biochem. Biophys. 211*, 227−233.
26. Pai, E. F., Karplus, P. A., and Schulz, G. E. (1988) *Biochemistry 27*, 4465−4474.
27. Bruns, C. M., and Karplus, P. A. (1995) *J. Mol. Biol. 247*, 125−145.
28. Kaplan, N. O. (1960) in *The Enzymes* (Boyer, P. D., Lardy, H., and Myrbäck, Eds.) Vol. 3, pp 105−169, Academic Press, New York.
29. Kaplan, N. O., Ciotti, M. M., and Stolzenbach, F., E. (1956) *J. Biol. Chem. 221*, 833−844.
30. Anderson, B. M., and Kaplan, N. O. (1959) *J. Biol. Chem. 234*, 1226−1232.
31. Vermilion, J. L., and Coon, M. J. (1978) *J. Biol. Chem. 253*, 2694−2704.
32. Kurzban, G. P., and Strobel, H. W. (1986) *J. Biol. Chem. 261*, 7824−7830.
33. Inano, H., and Tamaoki, B. (1986) *Eur. J. Biochem. 155*, 485−489.
34. Iyanagi, T., Makino, N., and Mason, H. S. (1974) *Biochemistry 13*, 1701−1710.
35. Daff, S. N., Chapman, S. K., Turner, K. L., Holt, R. A., Govindaraj, S., Poulos, T. L., and Munro, A. W. (1997) *Biochemistry 36*, 13816−13823.
36. Narhi, L. O., and Fulco, A. J. (1986) *J. Biol. Chem. 261*, 7160−7169.
37. Murataliev, M. B., and Feyereisen, R. (1996) *Biochemistry 35*, 15029−15037.
38. Ortiz-Maldonado, M., Gatti, D., Ballou, D. P., and Massey, V. (1999) *Biochemistry 38*, 16636−16647.
39. Witteveen, C. F. B., Giovanelli, J., Yim, M. B., Gachhui, R., Stuehr, D. J., and Kaufman, S., (1998) *Biochem. Biophys. Res. Commun. 250*, 36−42.
40. Noble, M. A., Munro, A. W., Rivers, Robledo, L., Daff, S. N., Yellowlees, L. J., Shimizu, T., Sagami, I., Guillemette, J. G., and Chapman, S. K. (1999) *Biochemistry 38*, 16413−16418.
41. Presta, A., Weber-Main, A. M., Stankovich, M. T., and Stuehr, D. J. (1998) *J. Am. Chem. Soc. 120*, 9460−9465.
42. Blankenhorn, G. (1975) *Eur. J. Biochem. 50*, 351−356.
43. O'Farrel, P. A., Walsh, M. A., McCarthy, A. A., Higgins, T. M., Voordouw, G., and Mayhew, S. G. (1998) *Biochemistry 37*, 8405−8416.
44. Peake, S. J., Venning, J. D., Cotton, N. P. J., and Jackson, J. B. (1999) *Biochim. Biophys. Acta 1413*, 81−91.
45. Boyer, P. D. (1997) *Annu. Rev. Biochem. 66*, 717−749.

BI992917K